Structural deformations and current oscillations in armchair-carbon nanotube cross devices: a theoretical study

Structural deformations and current oscillations in armchair-carbon nanotube cross devices: a theoretical study

A Kashefian Naieni, P Yaghoobi, D J Woodsworth and A Nojeh

Department of Electrical and Computer Engineering, The University of British Columbia,
Vancouver BC, V6T 1Z4, Canada

E-mail: anojeh@ece.ubc.ca

Abstract

A carbon nanotube (CNT) cross is a structure consisting of two CNTs with one draped over the other at an angle. Because of the localized mechanical deformation induced at the intersection point, the electronic properties of the nanotubes in a cross could vary significantly compared with those of intact nanotubes, potentially leading to the formation of nanoscale quantum dots.

Using classical molecular dynamics, we determined the relaxed nanotube structures and the induced mechanical deformations in a CNT cross. We found that the final relaxed shape of the cross structure is relatively insensitive to the starting shape. We then calculated the electronic transport properties of this device using a first-principles, non-equilibrium Green's function approach. We obtained current oscillations that can be attributed to the formation of a nanoscale quantum dot in the top nanotube at the intersection region.

(Some figures in this article are in colour only in the electronic version)

1. Introduction

Because of their remarkable properties, carbon nanotubes (CNTs) have attracted considerable attention over the past two decades. Their extremely small diameter (down to less than a nanometre), combined with lengths that can be on the order of hundreds of micrometres or even millimetres, as well as the rich variety of their electronic properties, all make CNTs promising candidates for building quantum electronic devices.

A CNT cross is a structure made of two CNTs crossing each other. The mechanical alterations induced in each nanotube in this structure make their electrical and electronic properties different from those of a straight CNT. Since the intersection area of the two CNTs is very small and thus the change in the mechanical and electronic properties is highly localized [1, 2], quantum confinement is expected to play a crucial role in electron transport through this structure, even at room temperature. The relationship between mechanical deformation and change in the electronic properties of CNTs has been studied both by simulation [3–8], and also experimentally [9, 10]. Strain can increase or decrease the band gap of semiconductive CNTs depending on

their chirality. The band gap of metallic zigzag tubes opens up under strain but armchair tubes are more stable. Cross sectional deformation of CNTs can result in semiconductor–metal or metal–semiconductor transitions in different tubes. Although no transition occurs as a result of uniform bending, at higher angles, bending can result in kinks that can cause severe localized alterations in the electronic properties of a tube (for a detailed description see [11]).

The top CNT in a cross structure is subject to all of the above mechanical perturbations. Although there have been experimental efforts to investigate the electronic modifications of the top CNT in the cross structure using scanning tunnelling microscopy [1, 12], a thorough simulation study can help us understand the properties of this structure better. We have previously explored the potential of this structure as a quantum device by showing the nanoscale nature of the electronic confinement [2].

In this paper, we report a simulation study of electronic transport through an armchair nanotube in a cross structure and compare it with that in a straight nanotube. The study was done for two different armchair nanotubes—(5,5) and (6,6). We used molecular dynamics (MD) simulations to determine

the physically viable configurations of a relaxed CNT cross. First-principles simulations were then used to calculate the effect of the resulting mechanical deformation of the top CNT on its electronic properties. Transport simulations through the nanotubes were performed using a Green's function-based approach to obtain the current–voltage characteristics of the devices.

2. Methodology

To determine the relaxed geometry of the CNT cross structure, MD simulations with adaptive intermolecular reactive empirical bond order (AIREBO) potentials [13] were performed using the NANOHIVE-1 software [14]. These potentials are well established for modelling intermolecular interactions in condensed-phase hydrocarbon sets. A real nanotube cross device would typically be lying on a substrate such as silicon or amorphous silicon dioxide. However, due to the difficulty of simulating such substrates, instead we used a graphene sheet as substrate. This seems to be a reasonable approximation due to the similar nature of the forces (Van der Waals) between a nanotube and graphene or silicon or oxide. Moreover, Hertel *et al* have shown that the calculated van der Waals binding energy of a CNT on a graphene sheet is in good agreement with the experimental values found for the binding energy of CNTs on a passivated silicon surface [15]. In addition, our main focus is on the qualitative study of the device behaviour, rather than exact, quantitative prediction. Lastly, we studied a wide range of deformations and our results can also provide insight into what to expect if substrates with different strengths of interaction with nanotubes are used.

The CNTs were placed perpendicular to each other and the top CNT was parallel to the zigzag edge of the graphene sheet. For the simulations, the bottom nanotube was initially placed parallel to the graphene substrate at a distance of 3.3 Å, which is the separation between graphene sheets in graphite. The position of this nanotube turned out to be quite steady during the simulations because of Van der Waals forces with the substrate. Since the intermolecular interactions in the AIREBO potentials are relatively short range, and also in order to reduce the simulation time, the geometry of the top nanotube was initially modified to be as close as possible to the expected final shape. Based on the available experimental reports of the top CNT profile in a cross structure using atomic force microscopy (AFM) [12, 15, 16], a Gaussian mapping was chosen as a good approximation of the top CNT profile. Two variables that needed to be determined for the mapping function were its height and full width at half maximum (FWHM). FWHM quantifies the length of the section of the top CNT which is not in contact with the substrate. The height was calculated by adding the bottom CNT diameter, the distance between the bottom CNT and the substrate, and the distance between the top and bottom CNTs (both were assumed to be 3.3 Å, as justified above). Unlike for the height, there is no preferred value for the FWHM and it can be set arbitrarily as long as the top nanotube is on (and not in) the bottom one. Experimentally, the initial FWHM depends on how the top nanotube first falls on the substrate, which can be different

in different cases. To cover various practical situations and investigate the effect of the initial extension of the top nanotube above the substrate, we performed simulations for different values of FWHM (28, 56, 84 Å). During MD simulations, the middle part of the top CNT started to bounce on the bottom one while its ends were fixed on the substrate due to Van der Waals forces. In the absence of a strong damping mechanism, these oscillations would continue for a long time. One way to change this situation towards a relaxed structure was to set the velocity of the atoms to zero at a certain moment—which we will call the freezing moment from now on—and then let the structure relax again. We will discuss this point in more detail later.

First-principles simulations were performed to find the change in the electronic structure of the top nanotube as a result of its structural deformation. Since these simulations are computationally very expensive, the number of atoms that can be included in the simulation is limited. The intersection area between the two nanotubes experiences the most deformation as compared with other parts of the CNT. Therefore, for electronic structure calculations on the top CNT, only the intersection area and a few adjacent unit cells on each side were included and the effects of the bottom nanotube and the substrate were not considered. The length of the nanotubes which were simulated was 22.6 Å (in the straight form) and the number of atoms was 200 and 240 for the (5,5) and (6,6) nanotubes, respectively. Vitalli *et al* [1] have also demonstrated that the drastic changes in the electronic properties of CNTs in a cross configuration happen in the crossing region and its close vicinity; the nanotube restores its characteristics (semiconducting in the particular case investigated in [1]) slightly away from the intersection. This further justifies our closer attention to the intersection area. Dangling bonds at each side were terminated with hydrogen atoms. The hydrogen atoms were relaxed, while the carbon atoms were kept fixed, using the Gaussian 09 software package [17]. The same software was used for density functional theory (DFT) simulations (using the B3LYP exchange-correlation functional with the 6-31G(d) basis set) for a range of applied electrostatic fields. The electric potential distribution in the structure (excluding the hydrogen atoms) was extracted and used in creating a three-dimensional, real space Hamiltonian. In simulation of nanotubes with the mentioned method (or other similar approaches), one should be careful about the effect of the hydrogen atoms added to cancel the dangling bonds. We tried to reduce their effects by simulating a sufficiently long portion of the nanotube and cutting out the hydrogen section when extracting the potential grid.

The transmission probability of electrons at different energies was calculated using a non-equilibrium Green's function approach with the above Hamiltonian built in a real-space basis. The self-energy terms were calculated using the method described by Appelbaum *et al* [18]. The magnitude of the current in the device at room temperature at different applied electric potentials was calculated using the Landauer–Buttiker formula [19]:

$$I = \frac{2q}{h} \int T(E)[f_1(E) - f_2(E)]\, dE. \tag{1}$$

2

In the above, $f_1(E)$ and $f_2(E)$ are the Fermi distribution functions of the contacts, $T(E)$ is the transmission of the channel at energy E, q is the charge of an electron and h is Planck's constant. The detailed description of the current calculation method has been presented in [20].

It is noteworthy that although electron–electron interactions are considered in the energies calculated using the DFT method, Coulomb blockade is not explicitly taken into account in the electronic wave functions and thus not fully included in our treatment.

3. Results and discussion

MD simulations with different initial configurations were performed for both nanotubes ((5,5), (6,6)). All MD simulations were performed at 1 K and with a 0.5 fs time step. An important question was how to choose the freezing moment (as defined above) and how it affects the final relaxed geometry of the CNT cross. To find a relaxed structure, an MD simulation, without any freezing, was first performed for each structure. The potential energy of the system was tracked as a function of time to find the moment at which the system has the minimum energy. The simulation was then re-run from the beginning, except the velocities of the atoms were manually set to zero at the freezing moment (the simulation step when the system has the minimum energy, as found above) and the structure was left to relax further. At the freezing moment, the structure was almost relaxed and the atoms moved only a very small amount during the subsequent relaxation. Structures with different initial FWHMs but freezing moments chosen using this process resulted in highly similar final relaxed configurations. The maximum height of the top nanotube reduced to 17.9 Å from the initial value of 20.2 Å for the (5,5) and to 19.6 Å from 22.8 Å for the (6,6) structure.

The obtained structure is not necessarily the one with the global minimum of energy; however, it is one likely relaxed configuration. To gain further insight we did another simulation with a freezing moment chosen at a point considerably different from the time when potential energy is at its minimum. This time, the final relaxed structure was noticeably different from the first one, with a significantly higher potential energy. Figure 1 shows the initial structure with FWHM equal to 56 Å and two structures relaxed under the two conditions mentioned. The structure in figure 1(*c*) has a kink but figure 1(*b*) is just deformed at the intersection.

Figure 2 shows the change in the energy of the structure as a function of time during the MD simulations. As is shown, structures with different initial FWHMs go towards essentially the same minimum final energy if the freezing moment is chosen in the same manner for all of them, but changing the freezing moment can lead to a different structure.

The freezing moment can provide one way of incorporating the effect of the environment on the structure while it is relaxing. If the structure has the chance to go towards its global minimum energy (for example if there is enough thermal energy during relaxation), regardless of how the top nanotube touches the substrate at first during nanotube deposition or growth, the relaxed structure would be the same
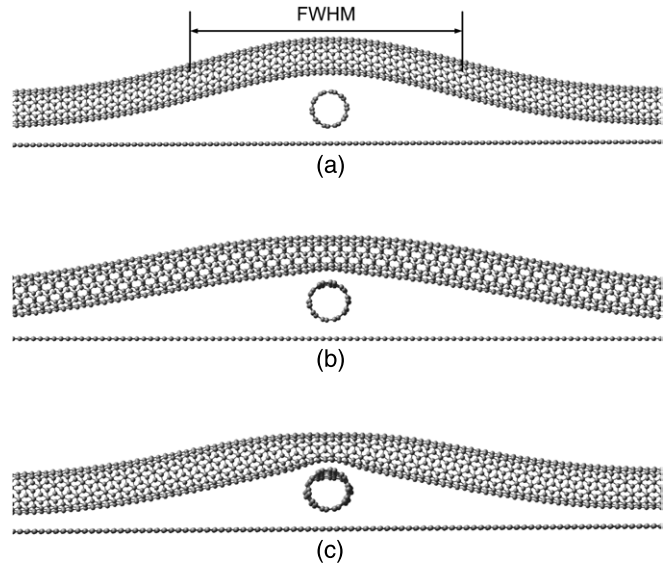

Figure 1. (*a*) The initial structure with FWHM of the Gaussian profile equal to 56 Å. (*b*), (*c*) two relaxed (5,5) cross structures with different freezing moments. Freezing moment (*b*) at the time when minimum energy is reached, (*c*) before reaching minimum energy.

at the end. However, if there is not enough thermal energy, depending on the initial conditions, the structure could become trapped in a local energy minimum. As a final note on structure relaxation, it is worth mentioning that we also performed similar MD studies on (8,0) and (9,0) (zigzag) nanotubes and found very similar results: if the freezing moment was calculated and used as described above, the final structure was quite insensitive to the initial configuration.

After obtaining the relaxed structure, we proceeded to investigate the electronic transport characteristics of the top nanotube. Figure 3 shows the current–voltage characteristics for (5,5) and (6,6) CNTs , calculated using our transport solver described in section 2.

As seen in figure 3, the current experiences an overall decrease as the deformation increases. The current through a straight nanotube increases with voltage starting at small voltages. In the case of the deformed tubes, there seems to be a voltage threshold below which the current is very low. Above the threshold, current increases with voltage in an almost monotonic fashion. However, a closer look at the current–voltage characteristics of the kinked structures reveals current oscillations with significantly higher relative strength than those observed in straight nanotubes (figure 4).

In an actual device made of metallic nanotubes, most of the voltage drop would be expected to be across the deformed region, with very little drop across the intact regions of the CNT. That is why we chose the upper limit of the applied voltage range to be in the order of a few volts (corresponding to typical voltages applied to such nanotube devices). The straight nanotube was simulated with the same voltages so we can compare the results.

Here a note is in order on thermal effects and electron–phonon interactions, which we have not taken into account. The ranges of voltages and currents in our simulations are within a few volts and several microamperes, which correspond
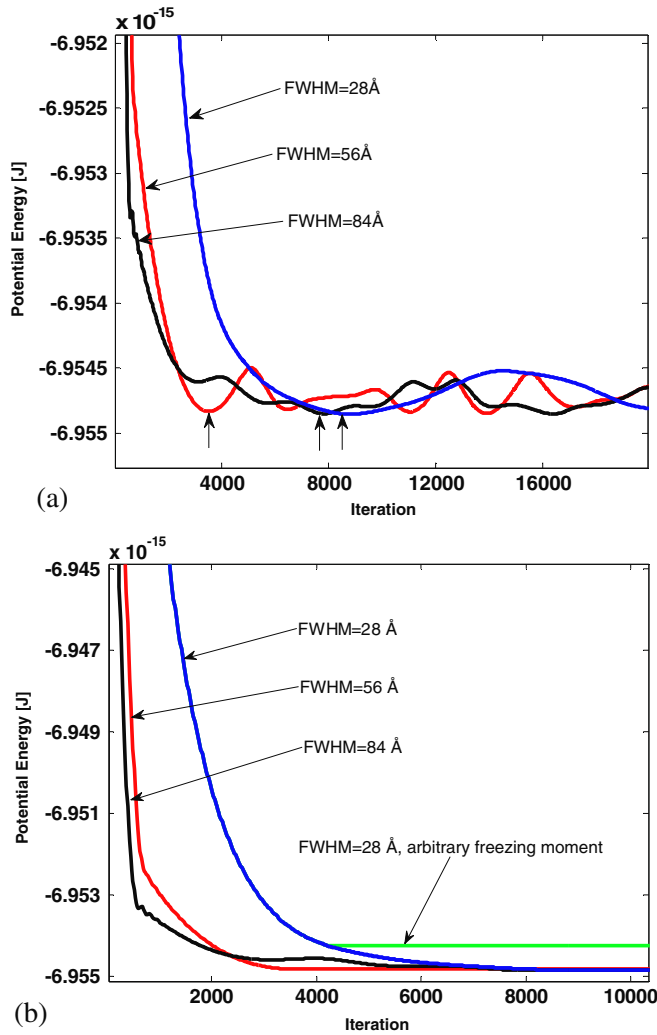
Figure 2. Potential energy of the (5,5) structure with different initial FWHMs as a function of time (*a*) without freezing (arrows show the freezing moments for the next round of simulation) and (*b*) with freezing the structure. Every iteration time step is 0.5 fs.

Figure 3. Current–voltage characteristics for straight, deformed and kinked CNTs: (*a*) (5,5) and (*b*) (6,6) CNTs.

to the experimental reality of nanotube devices. The rise in the nanotube temperature due to such levels of power dissipation is typically low enough that nanotube failure due to heating is not a major concern in our study. As a result, although self-heating of the CNT is not considered in these simulations, we believe it would not change the results drastically and that the trends would still be the same had it been taken into account. CNT–substrate interaction aids heat dissipation and so the current–voltage characteristics of CNTs lying on a substrate are not affected by thermal energy generation as much as is the case for suspended nanotubes [21]. Nonetheless, we expect that electron–phonon interactions become more important, and our results become less accurate, as the applied voltage is increased (the far-right side of the *I–V* characteristics of figures 3 and 4).

The current oscillations of figure 4 resemble those of a resonant tunnelling diode: indeed these oscillations seem to be due to quantized energy levels entering the energy range between the Fermi levels of the two contacts. The oscillations in the kinked (5,5) CNT are closer to each other than are those of the kinked (6,6) nanotube. To explain this, we note that
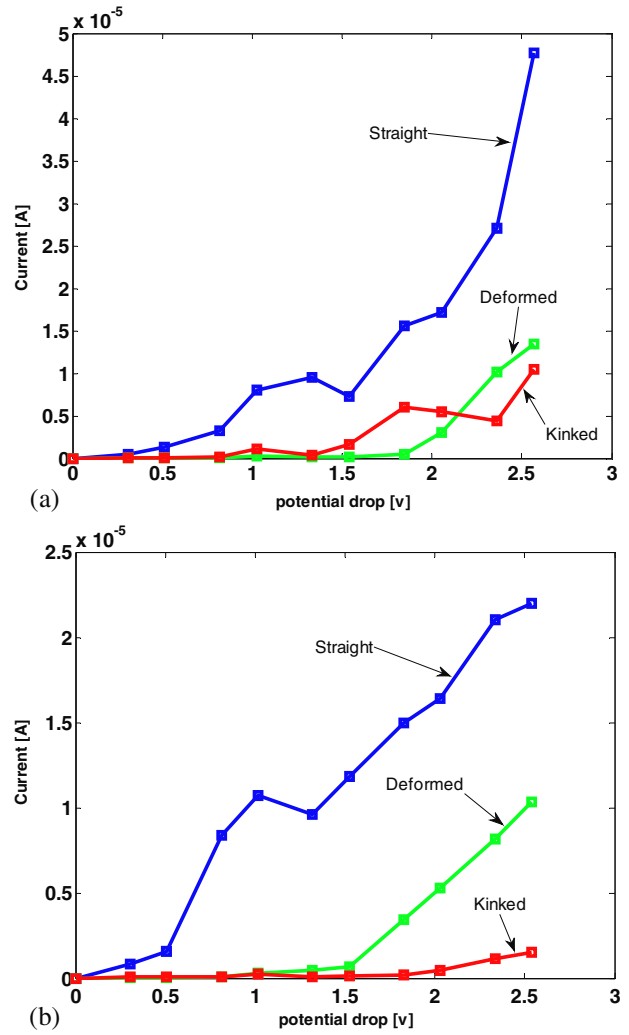
nanotubes with larger diameters show less rigidity and become deformed more easily [15]. This results in a more localized deformed region in a (6,6) cross and since the difference between the allowed energy levels is inversely related to the size of the confinement region, the current oscillations in a (6,6) nanotube are spaced further apart than the ones in a (5,5) nanotube.

To investigate the origin of these oscillations we explored the electron density profile along the top CNT. Using the *ab initio* simulation results, the electron density on a three-dimensional grid was extracted. Summing the values of the points on each cross sectional plane gives us an estimate of how the electron density varies along the nanotube (shown as dots in figure 5). This figure shows the electron density for the straight, deformed and kinked cases ((6,6) nanotube) plotted using this scheme.

As can be seen, there is overall electron depletion in the intersection area in the top nanotube as a result of deformation. This effect becomes stronger as the deformation increases and the nanotube is kinked. The Mulliken charge distribution (figure 6) shows a clearly positive region in the intersection area, especially on the squeezed side. This depleted area is the
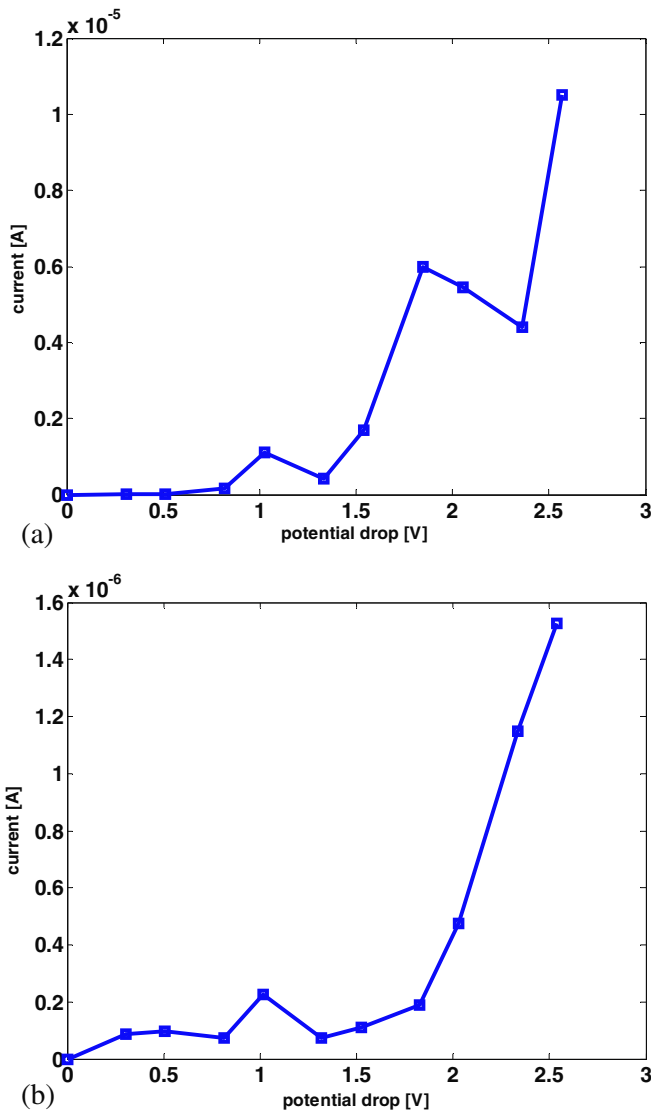
Figure 4. Magnified view of the current–voltage characteristics of kinked CNTs: (*a*) (5,5) and (*b*) (6,6).

Figure 5. Electron density profile along a (*a*) straight, (*b*) deformed and (*c*) kinked (6,6) top CNT in a cross structure (excluding the hydrogen atoms used for elimination of dangling bonds) derived as explained in the text. The red line shows an average of the dots. The horizontal axis demonstrates the grid points along the CNT.

main reason for the special current–voltage behaviour of the top nanotube in the cross structure. This area acts as a restricted p-type region between two metallic nanotube contacts. As a result, the potential energy landscape in this structure is very similar to that of two back-to-back diodes.

The crossing between the curves corresponding to deformed and kinked CNTs in figure 3(*a*) can be explained by better alignment of energy levels in the depleted region with states in the contacts in one versus the other case at different applied voltages. For the kinked nanotube, the better alignment happens at 1.8 V, leading to a peak at this voltage and a subsequent decrease, whereas for the deformed one this is not the case and the current starts increasing beyond 1.8 V. The overall effect is that the two curves intersect at around 2.1 V.

It should be noted, however, that such a simple 1D description cannot explain the results entirely because of the complex, 3D nature of the variations of quantities like the electron density in the actual structure. To gain further insight into the device behaviour and its current–voltage
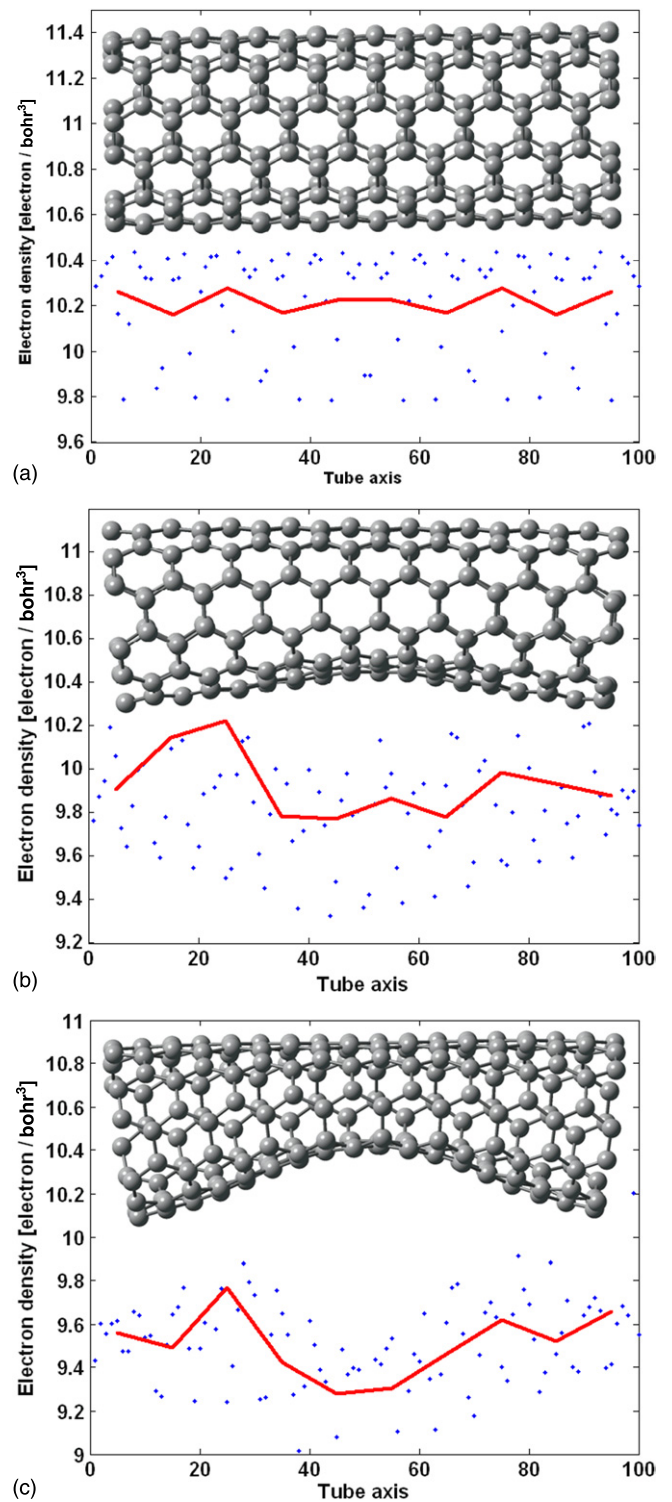
characteristics, we investigated the molecular orbitals of the top nanotube at different energies to evaluate how their shapes varied and how these shapes in turn affected the current–voltage characteristics. At higher applied voltages, the energy window between the Fermi levels of the contacts is larger
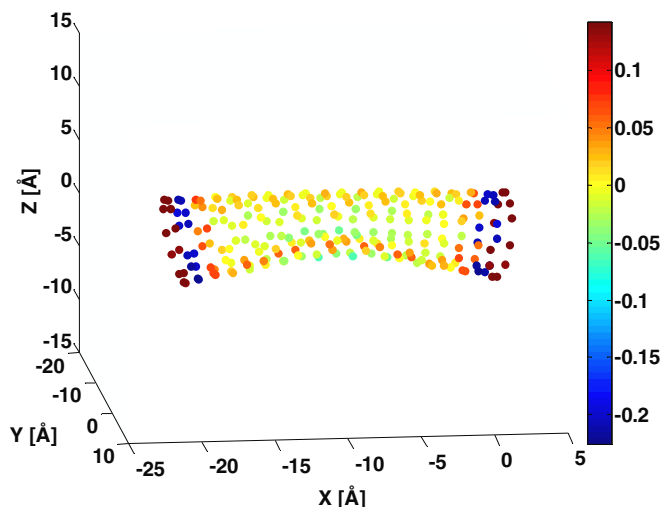
5

Figure 6. Mulliken charge distribution in a kinked (6,6) nanotube (colour bar is in atomic units).

Figure 7. Spatial distribution of the HOMO-2 orbital of a (*a*) straight and (*b*) kinked (5,5) nanotube. The kinked one shows a sparser coverage on the stretched part and a denser coverage on the squeezed part compared with the straight nanotube.

and more energy levels can contribute to the current. If the reason behind the oscillations in the current–voltage diagram is resonant tunnelling then the peaks must correspond to some of the energy levels. The current peaks at 1 V in figure 4(*a*) and (*b*) are examples of this effect. Another example is the second peak in the current–voltage characteristics of the kinked (5,5) structure that happens at around 1.8 V. At this voltage the window between the Fermi levels covers from −4.8 to −3 eV. The HOMO-2 orbital (where HOMO denotes the highest occupied molecular orbital), with an energy of −4.8 eV, enters the region between the Fermi levels of the contacts for the first time. Figure 7 shows this molecular orbital for both the straight and kinked cases. The straight nanotube orbital covers the whole body uniformly. In the kinked structure the coverage on the stretched part is sparse while the orbital covers the squeezed part (lower side of the nanotube) almost uniformly and much more densely compared with the lower side of the straight nanotube. This high coverage provides a strong conduction path, which leads to the corresponding current peak. In other words, the shapes of the orbitals suggest that current peaks in the kinked structure occur when the energy of an orbital with a high spatial coverage around the squeezed part of the tube comes between the Fermi levels of the contacts. Of course this effect is not as obvious in all orbitals and what really determines the electrical behaviour is the aggregate effect of all the orbitals. Nonetheless, this example gives us insight into the transport mechanism.

For larger armchair nanotubes, a more localized deformation is expected because of their lower rigidity, which would result in higher separation between quantum energy levels in the deformed region. Zigzag nanotubes have been shown to be stiffer against becoming kinked compared with armchair nanotubes [8], but at the same time they are more sensitive to mechanical alterations [5]. Overall, in all the cases, because of the extremely small size of the region that is considerably affected in a cross structure, quantum effects are expected to play a major role in electronic transport, independently of the size and chirality of the host nanotube. These effects ar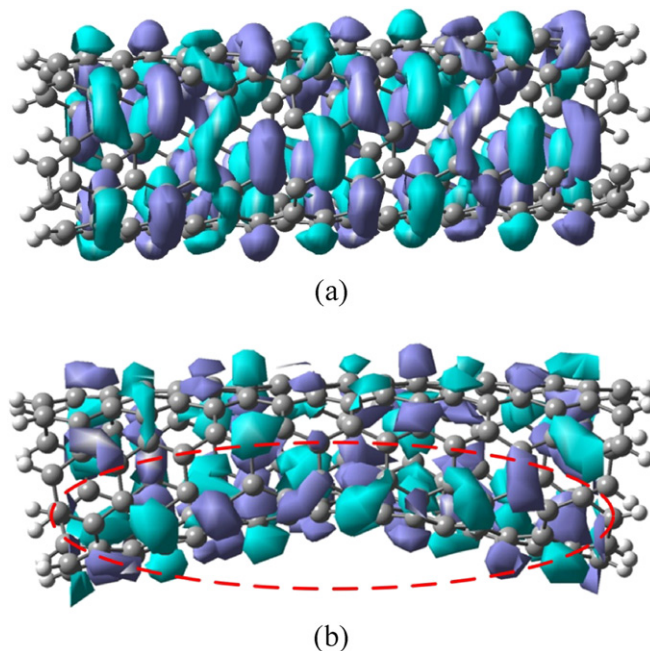e expected to be observable even at room temperature. Depending on the strength of the various mechanical perturbations (strain, cross sectional deformation and bending), the extract results would vary in each case.

4. Conclusions

Carbon nanotube cross structures consisting of armchair nanotubes were investigated. Molecular dynamics simulations showed that there exist multiple viable structures. Depending on the chosen process for relaxing the structure, different relaxed structures can be obtained. If the structure is frozen at its lowest energy point during simulation, the final structure is independent of the initial one.

Room temperature current–voltage characteristics of the top CNT in the cross show drastic changes in comparison with a straight nanotube. Current is suppressed at low voltages and shows oscillations at higher bias values. Investigation of the top nanotube reveals that there is partial electron depletion in the intersection region and that area acts like a carrier confining well. When the allowed energy levels of this confined region enter the energy range between the Fermi energies of the contacts, the current increases significantly, resulting in oscillations in the current–voltage characteristics. These oscillations indicate the probable presence of a quantum dot in the cross structure.

Acknowledgments

J. Phys. D: Appl. Phys. **44** (2011) 085402

A Kashefian Naieni *et al*

computing resources provided by WestGrid, SHARCNET and Compute/Calcul Canada.

References

[1] Vitali L, Burghard M, Wahl P, Schneider M A and Kern K 2006 Local pressure-induced metallization of a semiconducting carbon nanotube in a crossed junction *Phys. Rev. Lett.* **96** 086804

[2] Nojeh A, Lakatos G W, Peng S, Cho K and Pease R F W 2003 A carbon nanotube cross structure as a nanoscale quantum device *Nano Lett.* **3** 1187–90

[3] Nishidate K and Hasegawa M 2008 Universal band gap modulation by radial deformation in semiconductor single-walled carbon nanotubes *Phys. Rev.* B **78** 195403

[4] Mehrez H, Svizhenko A, Anantram M P, Elstner M and Frauenheim T 2005 Analysis of band-gap formation in squashed armchair carbon nanotubes *Phys. Rev.* B **71** 155421

[5] Shan B, Lakatos G W, Peng S and Cho K 2005 First-principles study of band-gap change in deformed nanotubes *Appl. Phys. Lett.* **87** 173109

[6] Nardelli M B and Bernholc J 1999 Mechanical deformations and coherent transport in carbon nanotubes *Phys. Rev.* B **60** R16338–41

[7] He Y, Zhang C, Cao C and Cheng H 2007 Effects of strain and defects on the electron conductance of metallic carbon nanotubes *Phys. Rev.* B **75** 235429

[8] Farajian A A, Yakobson B I, Mizuseki H and Kawazoe Y 2003 Electronic transport through bent carbon nanotubes: Nanoelectromechanical sensors and switches *Phys. Rev.* B **67** 205423

[9] Minot E D, Yaish Y, Sazonova V, Park J, Brink M and McEuen P L 2003 Tuning carbon nanotube band gaps with strain *Phys. Rev. Lett.* **90** 156401

[10] Gomez-Navarro C, Saenz J J and Gomez-Herrero J 2006 Conductance oscillations in squashed carbon nanotubes *Phys. Rev. Lett.* **96** 076803

[11] Kashefian Naieni A and Nojeh A 2010 Quantum dot devices based on carbon nanotubes *Nanoelectronics: Nanowires, Molecular Electronics, and Nanodevices* ed K Iniewski (New York: McGraw-Hill)

[12] Janssen J W, Lemay S G, Kouwenhoven L P and Dekker C 2002 Scanning tunneling spectroscopy on crossed carbon nanotubes *Phys. Rev.* B **65** 115423

[13] Stuart S J, Tutein A B and Harrison J A 2000 A reactive potential for hydrocarbons with intermolecular interactions *J. Chem. Phys.* **112** 6472–86

[14] Helfrich B 2005 *Nanohive-1, v.1.2.0-b1.* (Nanorex, Inc.)

[15] Hertel T, Walkup R E and Avouris P 1998 Deformation of carbon nanotubes by surface van der Waals forces *Phys. Rev.* B **58** 13870–3

[16] Ismach A and Joselevich E 2006 Orthogonal self-assembly of carbon nanotube crossbar architectures by simultaneous graphoepitaxy and field-directed growth *Nano Lett.* **6** 1706–10

[17] Frisch M J et al 2009 *Gaussian 09, Revision A.02* (Wallingford, CT: Gaussian, Inc.)

[18] Appelbaum I, Wang T, Joannopoulos J D and Narayanamurti V 2004 Ballistic hot-electron transport in nanoscale semiconductor heterostructures: Exact self-energy of a three-dimensional periodic tight-binding Hamiltonian *Phys. Rev.* B **69** 165301

[19] Datta S 2002 *Electronic Transport in Mesoscopic Systems* (Cambridge: Cambridge University Press)

[20] Yaghoobi P, Walus K and Nojeh A 2009 First-principles study of quantum tunneling from nanostructures: current in a single-walled carbon nanotube electron source *Phys. Rev.* B **80** 115422

[21] Pop E, Mann D, Cao J, Wang Q, Goodson K and Dai H 2005 Negative differential conductance and hot phonons in suspended nanotube molecular wires *Phys. Rev. Lett.* **95** 155505